Proc. Natl. Acad. Sci. USA
Vol. 96, pp. 238–241, January 1999
Medical Sciences

Toward a cancer therapy with boron-rich oligomeric phosphate diesters that target the cell nucleus

AKIRA NAKANISHI*†, LUFENG GUAN†‡, ROBERT R. KANE‡§, HARUMI KASAMATSU*, AND M. FREDERICK HAWTHORNE‡¶

Departments of ‡Chemistry and Biochemistry and *Molecular, Cell, and Developmental Biology and the Molecular Biology Institute, University of California, 405 Hilgard Avenue, Los Angeles, CA 90095

Contributed by M. Frederick Hawthorne, November 2, 1998

ABSTRACT **The viability of boron neutron capture therapy depends on the development of tumor-targeting agents that contain large numbers of boron-10 (^{10}B) atoms and are readily taken up by cells. Here we report on the selective uptake of homogeneous fluorescein-labeled *nido*-carboranyl oligomeric phosphate diesters (*nido*-OPDs) by the cell nucleus and their long-term retention after their delivery into the cytoplasm of TC7 cells by microinjection. All *nido*-OPDs accumulated in the cell nucleus within 2 h after microinjection. However, *nido*-OPDs in which the carborane cage was located on a side chain attached to the oligomeric backbone were redistributed between both the cytoplasm and nucleus after 24 h of incubation, whereas *nido*-OPDs in which the carborane cage was located along the oligomeric backbone remained primarily in the nucleus. Furthermore, cell-free incubation of digitonin-permeabilized TC7 cells with the *nido*-OPDs resulted in nuclear accumulation of the compounds, thus corroborating the microinjection studies. Our observation of fluorescence primarily located in the cell nucleus indicates that nuclear-specific uptake of sufficient amounts of ^{10}B for effective boron neutron capture therapy ($\approx 10^8$–10^9 ^{10}B atoms/tumor cell) via *nido*-OPDs is achievable.**

Boron neutron capture therapy (BNCT) is a binary radiation therapy for cancer, which entails the capture of thermal neutrons by boron-10 (^{10}B) nuclei that have been selectively delivered to tumor cells. The neutron capture event results in the formation of excited ^{11}B nuclei, which fission to yield highly energetic $^4He^{2+}$ and $^7Li^{3+}$ ions. Cell death is triggered by the release of these charged particles that create ionization tracks along their trajectories, resulting in cellular damage. Neighboring cells are generally spared because the range of the fission particles is only ≈1 cell diameter. Selective delivery to tumor of 10–30 μg ^{10}B/g of tumor (1) is required for effective cytotoxicity with BNCT. By targeting the tumor cell nucleus, lower concentrations of boron are required for successful therapy because a single neutron–^{10}B capture event within tumor cell DNA would be lethal to the cell (2).

Modalities under development for the delivery of ^{10}B to tumor include porphyrins, monoclonal antibodies, nucleosides, amino acids, and liposomes (1, 3). Of major importance in determining the efficacy of any of these delivery vehicles is the resulting subcellular localization of the boron. Recently, a number of homogeneous *nido*-carboranyl oligomeric phosphate diesters (*nido*-OPDs) have been developed that selectively accumulate in EMT6 tumors grown in BALB/c mice (unpublished results), but the mechanism of transport of these *nido*-OPDs across the plasma membrane is unknown. Subcellular localization of these *nido*-OPDs has not been previously investigated and appeared to merit immediate examination because of their versatile structures, ready availability, and potential for specific cellular targeting with liposomes.

To explore possible subcellular boron localization by both *closo*- and *nido*-OPDs, microinjection studies and experiments with permeabilized cells were conducted. Microinjection and permeabilization of cells were used because of the inability of the OPDs to enter TC7 cells under culture conditions. TC7 cells, a subline of African green monkey kidney cells, were used in all experiments because of their apparent resilience to the process of microinjection and our desire to use a mammalian cell line. Microinjection studies were conducted to investigate the subcellular distribution of *closo*- and *nido*-OPDs in living cells. Although, the permeabilized cells were used to assess cell-free nuclear entry of *closo*- and *nido*-OPDs. (In such cells, the plasma membrane is selectively permeabilized, which releases the cytosol, yet leaves the nuclear envelope intact.) These two *in vitro* methods were used to document subcellular boron localization and investigate the localization mechanism.

METHODS

Preparation of OPDs. In brief, all OPDs (Fig. 1) were constructed from fluorescein-controlled pore glass (CPG) (Glen Research, Sterling, VA) and *closo*-CB and *closo*-G1 dimethoxytrityl-protected phosphoramidite monomers on automated DNA synthesis instruments (Midland Certified Reagent, Midland, TX). The synthesis of the CB dimethoxytrityl-protected phosphoramidite monomer has been described (4). The synthesis of the G1 dimethoxytrityl phosphoramidite monomer follows a similar route and will be described elsewhere. All *closo*-OPDs, once cleaved from the controlled pore glass support and, when desired, degraded to *nido*-carboranyl species with 30% ammonium hydroxide aqueous solution, were purified with Centrisep-3 membrane filters (Princeton Separations, Adelphia, NJ) and by RP-HPLC. Purity was determined by HPLC and PAGE. Finally, each OPD was converted to its sodium salt by ion exchange.

Subcellular Localization Studies. *Microinjection of OPDs and rhodamine-labeled dextran molecules.* Cell culture and microinjection procedures have been described (5). In brief, TC7 cells grown on marked coverslips (≈10^5 cells/coverslip) were transferred to Hepes-buffered medium (pH 7.4) and fluorescein-labeled boron-rich OPDs (5–100 μM) or rhodamine-labeled dextran molecules (1 mg/ml) in PBS were individually microinjected directly into the cytoplasm. In typical

Abbreviations: BNCT, boron neutron capture therapy; ^{10}B, boron-10; *nido*-OPD, *nido*-carboranyl oligomeric phosphate diester; *closo*-OPD, *closo*-carboranyl oligomeric phosphate diester; OPD, oligomeric carboranyl phosphate diester.

The publication costs of this article were defrayed in part by page charge payment. This article must therefore be hereby marked "*advertisement*" in accordance with 18 U.S.C. §1734 solely to indicate this fact.

†A.K. and L.G. contributed equally to the work.
§Present address: Department of Chemistry, Baylor University, Waco, TX 76798.
¶To whom reprint requests should be addressed. e-mail: mfh@chem.ucla.edu.

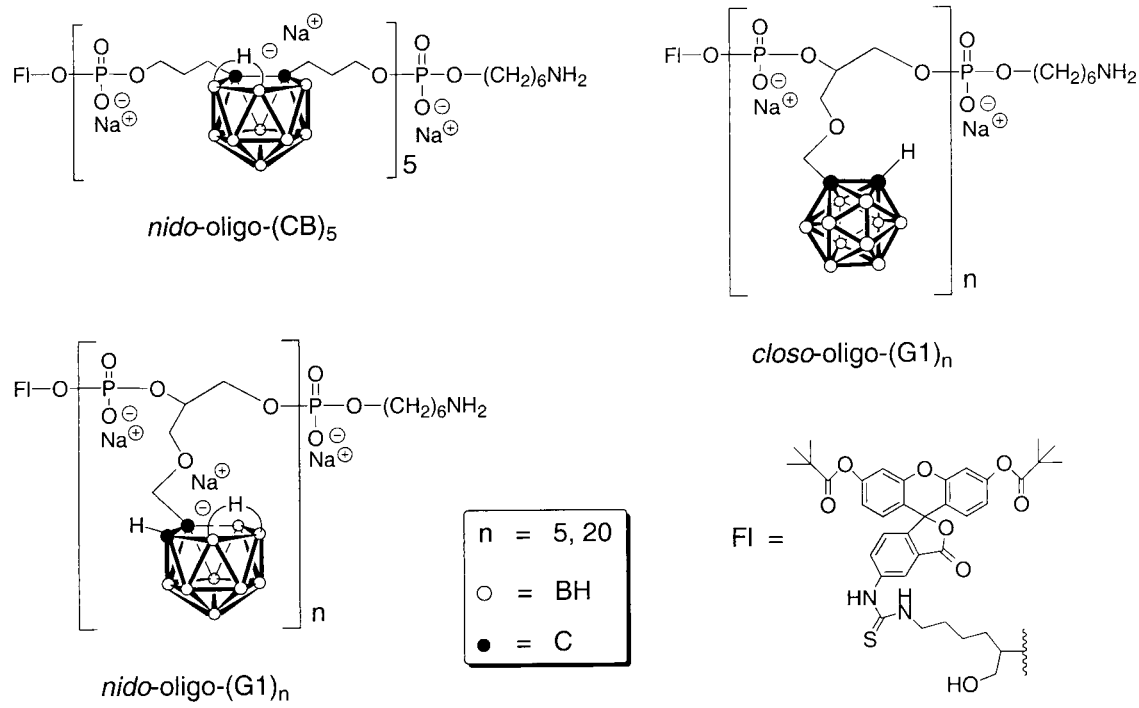

FIG. 1. The structure of the fluorescein-labeled *nido*-$(CB)_5$, *nido*-$(G1)_5$, and *closo*-$(G1)_5$.

microinjection experiments, approximately 10% of the cell volume, or 3.6×10^{-10} ml, can be injected into the cytoplasm (6). Assuming that all cells received the same volume, approximately 2.2×10^7 OPD ions (100 μM solution) were introduced into each cell [corresponding to 9.7×10^8 boron atoms from *nido*-$(CB)_5$ or *nido*-$(G1)_5$]. Once microinjected, the cells were incubated at 37°C for the designated time and were briefly washed with PBS. The fluorescein or rhodamine subcellular localization was immediately observed by epifluorescence microscopy without fixation. The conditions for phase contrast and epifluorescence microscopy are the same as those described (7).

Coinjection of nido-$(CB)_5$ and rhodamine-labeled BSA. The coinjection procedure is the same as the microinjection protocol described above. The microinjection sample consisted of a 1:1 solution of fluorescein-labeled boron-rich *nido*-$(CB)_5$ (5 μM) and rhodamine-labeled BSA (1 mg/ml) in PBS.

Permeabilized cells. The digitonin-permeabilization protocol is the same as that developed for the measurement of active protein import from the cytoplasm to the nucleus (8), except that the subsequent incubation with the OPD was performed in the absence of the cytosol and the ATP-regenerating system. Both are necessary for active transport, but their absence allows the study of diffusional entry of molecules into the nucleus (unpublished result). Briefly, TC7 cells were rinsed with cold buffer (20 mM Hepes, pH 7.3/110 mM potassium acetate/5 mM magnesium acetate/2 mM DTT/1 μg/ml each of aprotinin, pepstatin, and leupeptin) and then permeabilized with 40 μg/ml of digitonin in the buffer at 4°C for 5 min. After permeabilization, the coverslips were rinsed twice, inverted on 50 μl of the buffer containing 0.1 pmol/μl of each boron-rich OPD ($\approx 3 \times 10^7$ boron-containing ions/cell), incubated for 30 min at 37°C, and then rinsed with the buffer. The fluorescein signal was observed as described above.

Coculture of nido-$(CB)_5$ with TC7 cells. Cell culture procedures have been described (5). Briefly, a hollow polystyrene cylinder (8 mm × 4.7 mm i.d.) was placed on a coverslip with TC7 cells ($\approx 10^5$ cells/coverslip). After the replacement of the buffer medium inside the cylinder with 200 μl of fluorescein-labeled *nido*-$(CB)_5$/PBS solution (250 mM), the cells were incubated for 1 h at 37°C. The fluorescein signal was observed as described above.

RESULTS AND DISCUSSION

Because of their ability to selectively localize in tumor, homogeneous hydrophilic boron-rich *nido*-oligomeric phosphate diesters (*nido*-OPDs) are of particular interest in subcellular localization studies. These species contain large numbers of boron atoms per molecule, are stable under physiological pH (9), and are easily obtained from the corresponding *closo*-OPDs. Many *closo*-OPDs have previously been synthesized (10) with one negative charge in the phosphate portion of each repeating unit of the *closo*-OPD. Fluorescein-labeled *closo*-OPDs are easily converted to their more hydrophilic and identically labeled *nido*-OPDs, which carry an additional negative charge on their *nido*-carborane cages (Fig. 1; refs. 1, 3, and 4). Members of the two structurally different CB and G1 series of fluorescein-labeled OPDs, *nido*-$(CB)_5$, and both *closo*- and *nido*-$(G1)_5$, were studied for their ability to accumulate and be retained in the cell nucleus. The carborane cage in *nido*-$(CB)_5$ is di-C-substituted and constitutes part of the backbone of the oligomer, whereas the cage in both *closo*- and *nido*-$(G1)_5$ is mono-C-substituted and is attached to these oligomeric structures by side chains. The fluorescein-labeled OPDs are quite stable in either moderately acidic or basic conditions, and the fluorescein group is unlikely to be released from the oligomers under physiological conditions (11).

The cellular compartmentalization of these novel compounds was tested. Because the coculture of *nido*-$(CB)_5$ with TC7 cells did not result in nuclear or significant cytoplasmic uptake of compound, microinjection and cell-free studies were conducted. When fluorescein-labeled *nido*-$(CB)_5$ and rhodamine-labeled BSA were coinjected into the cytoplasm of the TC7 cells, *nido*-$(CB)_5$ localized in the nucleus (Fig. 2*a*) while the BSA remained in the cytoplasm (Fig. 2*b*). *Nido*-$(CB)_5$ was observed in the nucleus within 10 min after injection, demonstrating its rapid accumulation (Fig. 2*c*). Additionally, it was observed that this compound was retained in the nucleus for at least 24 h (Fig. 2*e*). In a separate experiment, rhodamine-

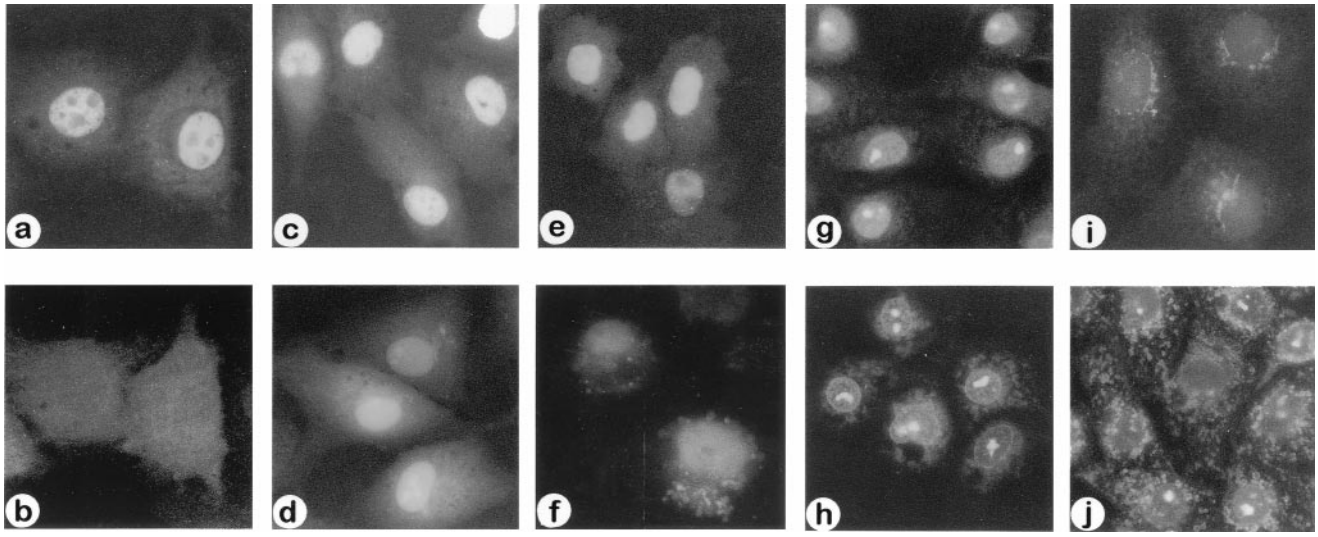

FIG. 2. Subcellular localization of fluorescein-labeled *nido*- and *closo*-OPDs *in vitro*. (*a* and *b*) The same set of cells 2 h after coinjection of *nido*-$(CB)_5$ (5 μM solution) and rhodamine-labeled BSA (1 mg/ml) into the cytoplasm. When viewed at their characteristic UV wavelengths, *nido*-$(CB)_5$ appears in the nucleus (*a*) and BSA appears in the cytoplasm (*b*). (*c* and *d*) Rapid nuclear accumulation of *nido*-$(CB)_5$ (100 μM solution) (*c*) and *nido*-$(G1)_5$ (100 μM solution) (*d*) within 10 min after cytoplasmic microinjection. (*e* and *f*) Long-term nuclear retention of *nido*-$(CB)_5$ (100 μM solution) (*e*) and *nido*-$(G1)_5$ (100 μM solution) (*f*) in the cells 24 h after cytoplasmic microinjection. (*g* and *h*) Distribution of OPD in subcellular compartments in digitonin permeabilized cells incubated with *nido*-$(CB)_5$ (*g*) and *nido*-$(G1)_5$ (*h*). (*i* and *j*) Subcellular distribution of *closo*-$(G1)_5$ in the cells 2 h after microinjection (100 μM solution) (*i*) and in digitonin permeabilized cells (*j*).

labeled inert dextran molecules (70 kDa) microinjected into the cytoplasm did not localize in the cell nucleus (not shown). The failure of both the large BSA (Fig. 2*b*) and the large dextran molecules to enter the nucleus suggests that small *nido*-$(CB)_5$ oligomers (2.7 kDa) enter the nucleus by diffusion.

The nuclear accumulation of *nido*-$(CB)_5$ also was demonstrated in cell-free studies by using permeabilized cells. When the plasma membrane of the cell was selectively permeabilized with digitonin followed by incubation with *nido*-$(CB)_5$, the accumulation of *nido*-$(CB)_5$ in the nucleus was again observed (Fig. 2*g*). This nuclear localization in the absence of cytoplasmic components essential for active nuclear transport also indicates diffusional entry of the *nido*-OPD.

Nuclear accumulation of *nido*-$(G1)_5$ after its microinjection into the cytoplasm and after its incubation under cell-free conditions was similar to that observed with *nido*-$(CB)_5$ for up to 2 h (Fig. 2, compare *c* and *d*, *g* and *h*; Table 1). However, differences in the location of the anionic carborane cage, whether along the OPD backbone, as in *nido*-$(CB)_5$, or on a side chain attached to the backbone, as in *nido*-$(G1)_5$, apparently affected the long-term intracellular distribution pattern (Fig. 2, compare *e* and *f* at 24 h). *Nido*-$(G1)_5$ redistributed in the cytoplasm and nucleus after 24 h of incubation (Fig. 2, compare *d* and *f*) while *nido*-$(CB)_5$ remained primarily in the nucleus (Fig. 2, compare *c* and *e*). The short-term subcellular localization of *nido*-$(G1)_{20}$ is similar to that of *nido*-$(G1)_5$ because it accumulates primarily in the nucleus (Table 1). The effect of the OPDs on cell growth during the microinjection studies should be noted. *Nido*-$(G1)_5$ was injected into 65 cells and *nido*-$(CB)_5$ was injected into 100 cells. After 24 h, 111 cells and 121 cells were present, respectively. Under phase-contrast microscopy, the injected cells maintained the same morphology as noninjected cells (Fig. 3), implying that cell growth is largely unaffected by the presence of the OPDs.

Table 1. Subcellular localization of fluorescein-labeled OPDs injected into the cytoplasm (360 pl of a 100-μM OPD solution)

Fluorescein-labeled oligomers	Subcellular localization	
	at $\approx$2 h	at $\approx$24 h
Fl-*nido*-$(CB)_5$	Nucleus	Nucleus
Fl-*nido*-$(G1)_5$	Nucleus	Nucleus/cytoplasm
Fl-*closo*-$(G1)_5$	Cytoplasm	Cytoplasm
Fl-*nido*-$(G1)_{20}$	Nucleus	ND
Fl-*closo*-$(G1)_{20}$	Cytoplasm	ND

ND, Not determined.

Uptake of $\approx 10^8$–10^9 randomly distributed ^{10}B atoms/tumor cell is necessary for effective BNCT. This number of ^{10}B atoms/cell was administered in these studies. In theory, lesser quantities could be used if the ^{10}B localized solely in the cell nucleus (2). Our observation that fluorescence is essentially confined to the nucleus indicates that nuclear-specific uptake of sufficient amounts of boron for effective BNCT via *nido*-OPDs is achievable.

In contrast to the distinct nuclear accumulation pattern of the *nido*-OPDs, the less hydrophilic *closo*-OPDs, *closo*-$(G1)_5$, and *closo*-$(G1)_{20}$ were distributed in both cytoplasmic and nuclear compartments *in vitro* (Fig. 2*i* and compare *h* and *j*; Table 1). The adherence of closo-OPDs to cytoplasmic components, possibly vesicular apparati, was prominent in permeabilized cells (Fig. 2*j*), but it also was observed after microinjection (Fig. 2*i*).

Aqueous channels in the nuclear pore complex allow diffusion of small molecules ($<$20–40 kDa) in and out of the nucleus (12). The *nido*-OPDs used in this study are sufficiently small (2.7–8 kDa) to diffuse into the nucleus, and their rapid accumulation there suggests that they have an affinity for nuclear components. Because the *nido*-OPDs contain two negative charges per repeating unit, they may bind to positively charged nuclear protein molecules, such as histones, and thus be retained in the nucleus. A small polyanionic species, dextran sulfate, has been shown to displace histones from both metaphase and interphase chromosomes in physiological salt conditions (13). Dextran sulfate also disrupts nuclear organization, resulting in the swelling and bursting of cell nuclei (14, 15). This was not observed in the *in vitro* studies with *nido*-OPDs reported here. Consequently, the interaction of *nido*-OPDs with nuclear constituents differs from that of dextran sulfate with histones, and its exact nature remains to be elucidated.

The selective affinity of hydrophilic *nido*-OPDs for the cell nucleus makes them very attractive as components of BNCT

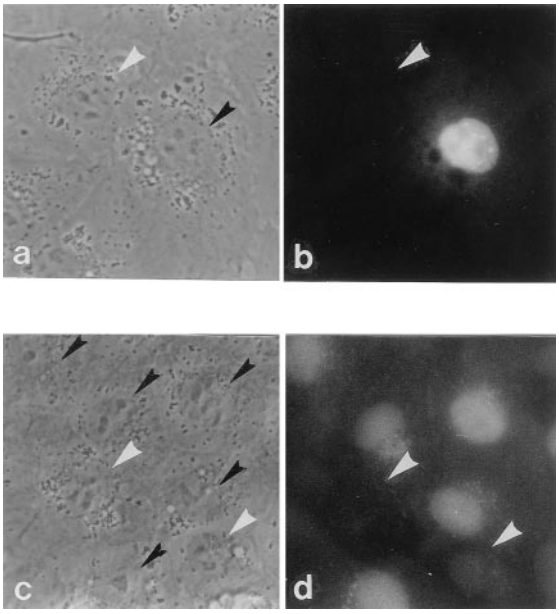

FIG. 3. Phase contrast and fluorescence micrographs of TC7 cells 24 h after cytoplasmic microinjection of either *nido*-$(CB)_5$ or *nido*-$(G1)_5$. (*a* and *b*) The same set of cells microinjected with *nido*-$(CB)_5$. (*c* and *d*) The same set of cells microinjected with *nido*-$(G1)_5$. Black arrowheads in phase contrast micrographs (*a* and *c*) indicate the nuclei of the cells microinjected with *nido*-OPDs. White arrowheads in phase contrast micrographs (*a* and *c*) and fluorescence micrographs (*b* and *d*) indicate the nuclei of the cells not microinjected with *nido*-OPDs.

agents. Encapsulation of *nido*-OPDs in tumor cell-targeted liposomes should circumvent the compounds' inability to penetrate the cell membrane and provide selective cell death. The relatively high concentration of *nido*-OPDs in the nucleus after its microinjection and long incubation period (24 h) appears to be influenced by the disposition of the anionic *nido*-carborane cages relative to the OPD chain. These subcellular distribution data suggest a structural selectivity in the extent to which various *nido*-OPDs bind to macromolecules in the nucleus. Selection of the optimum *nido*-OPD derivatives for BNCT thus will require a systematic examination of the nuclear accumulation of candidate species. This study indicates that the structure and function of the boron-rich *nido*-OPDs make them ideal candidates for the nuclear targeting and cellular retention required for boron neutron capture therapy.

We thank M. Smuckler for editing this manuscript. This work was supported by grants from the National Cancer Institute and a pilot fund from University of California, Los Angeles, Jonsson Comprehensive Cancer Center.

1. Hawthorne, M. F. (1993) *Angew. Chem. Int. Ed. Engl.* **32,** 950–984.
2. Hartman, T. & Carlsson, J. (1994) *Radiother. Oncol.* **31,** 61–75.
3. Soloway, A. H., Tjarks, W., Barnum, B. A., Rong, F.-G., Barth, R. F., Codogni, I. W. & Wilson, J. G. (1998) *Chem. Rev.* **98,** 1515–1562.
4. Kane, R. R., Drechsel, K. & Hawthorne, M. F. (1993) *J. Am. Chem. Soc.* **115,** 8853–8854.
5. Clever, J. & Kasamatsu, H. (1991) *Virology* **181,** 78–90.
6. Fung, B. (1984) Ph.D. thesis (University of California, Los Angeles).
7. Kasamatsu, H. & Nehorayan, A. (1979) *J. Virol.* **32,** 648–660.
8. Adam, S. A., Marr, R. A. & Gerace, L. (1990) *J. Cell Biol.* **111,** 807–816.
9. Primus, F. J., Pak, R. H., Rickard-Dickson, K. J., Szalai, G., Bolen, J. L., Jr., Kane, R. R. & Hawthorne, M. F. (1996) *Bioconjugate Chem.* **7,** 532–535.
10. Kane, R. R., Kim, Y. S. & Hawthorne, M. F. (1997) in *Advances in Neutron Capture Therapy. Volume II: Chemistry and Biology*, eds. Larsson, B., Crawford, J. & Weinreich, R. (Elsevier, New York), pp. 113–118.
11. Kumke, M. U., Li, G., McGown, L. B., Walker, G. T. & Linn C. P. (1995) *Anal. Chem.* **67,** 3945–3951.
12. Forbes, D. J. (1992) *Annu. Rev. Cell Biol.* **8,** 495–527.
13. Laemmli, U. K., Cheng, S. M., Adolph, K. W., Paulson, J. R., Brown, J. A. & Baumbach, W. R. (1978) *Cold Spring Harbor Symp. Quant. Biol.* **42,** 351–360.
14. Nakashima, A., Mori, K. & Sasaki, S. (1996) *Biochem. Biophys. Res. Commun.* **228,** 846–851.
15. Mori, K., Nakashima, A. & Sasaki, S. (1997) *Biochem. Biophys. Res. Commun.* **234,** 783–787.